Draft version August 18, 2018
Typeset using LaTeX **twocolumn** style in AASTeX62

The Green Bank Ammonia Survey: Investigation of the Hierarchical Structures of Nearby Star-Forming Regions

James Lilly[1,2] and Rachel Friesen[1]

[1] *National Radio Astronomy Observatory, 520 Edgemont Road, Charlottesville, VA 22903, USA*
[2] *Steward Observatory, University of Arizona, 933 North Cherry Avenue, Tucson, AZ 85721, USA*

ABSTRACT

We present an analysis of the hierarchical structures of the four star-forming regions (SFRs) included in the first data release (DR1) of the Green Bank Ammonia Survey (GAS). We detail our methods for optimizing a robust parameter set for the dendrogram technique used to map these hierarchical structures. We find that multiples of the median rms value extracted from the integrated intensity map (0^{th} moment) of each region are sufficient baselines for the dendrogram parameters, with respect to only identifying real structures. Finally, we present preliminary findings for each region on: a) minimal correlations between both structure size and aspect ratio & the relative orientations of small and large-scale structures b) the possibility of dendrograms identifying stellar/pre-stellar cores.

1. INTRODUCTION

Stars form in regions of dense gas characterized by a complex hierarchy of large-scale filaments (André et al. 2010) and smaller-scale cores located within those filaments. Mapping these regions, particularly at optical wavelengths, presents a number of challenges because of the cold and dusty environments in which they reside. GAS aimed to resolve these challenges by utilizing the high-sensitivity of the Green Bank Telescope, selecting an ideal gas tracer, and observing nearby Gould Belt regions ($d < 500$ pc). The central focus of this work is to map the hierarchical structure of the four star-forming regions in various molecular clouds (included in DR1 of GAS which are: NGC1333 in Perseus, Orion A North in Orion, B18 in Taurus, and L1688 in Ophiuchus.

The central challenge in mapping the hierarchical structure of these regions is to accurately trace this dense gas such that all components of the hierarchy are resolved and distinguishable from neighboring structures. GAS accomplished this by selecting NH_3 (ammonia) as its tracer. NH_3 is an excellent tracer for observing SFRs primarily because it does not freeze onto dust grains at low temperatures. In the case of star-forming regions, this is an important behavior as these environments are both cold and populated with significant amounts of dust. NH_3 is also an ideal tracer because it is rotationally excited by collisions within areas of dense gas, which allows for detailed spectral line observations at radio wavelengths, like those conducted with GAS. For more information on the details of the GAS observations, see Friesen et al. 2017.

To generate maps of each region's structural hierarchy, we applied a dendrogram analysis technique, courtesy of the *astrodendro* Python package, to the GAS DR1 data. Molecular gas is characteristically hierarchical (Rosolowsky et. al 2008) which makes dendrograms an apt tool for classifying the structural hierarchy of the DR1 regions. We applied this package to the integrated intensity (0^{th} moment) maps extracted from the data cubes made with GAS. These maps collapse the PPV (position-position-velocity) cubes along their velocity axis to associate each pixel with a flux which roughly corresponds to the column density along the pixel's line-of-sight. We conducted this dendrogram analysis on these maps in particular because, for this study, we were primarily concerned with the relative positions and intensities (fluxes) of structures within each region, therefore utilizing the full PPV cube would have added unnecessary complexity to our analysis. For example, NH_3 has a significant number of hyperfine components meaning that some "structure" may be detected multiple times if it is associated with several ammonia emission lines. There is also a risk associated with 0^{th} moment maps as, since they collapse the PPV cubes along their velocity axis, there may be multiple velocities along a particular line of sight that could potentially be two distinct structures which the dendrograms would not separate. However, Friesen et al. (2017) found that overall, most regions do not have multiple velocity components along the line-of-sight so the flux of each structure is more important to the dendrogram analysis than the velocity information.

By generating these dendrograms for each region, we characterized their structural make-ups by breaking them down into their small (leaves) and large-scale (trunks) components. Additionally, we developed a robust set of parameters for the *astrodendro* package that

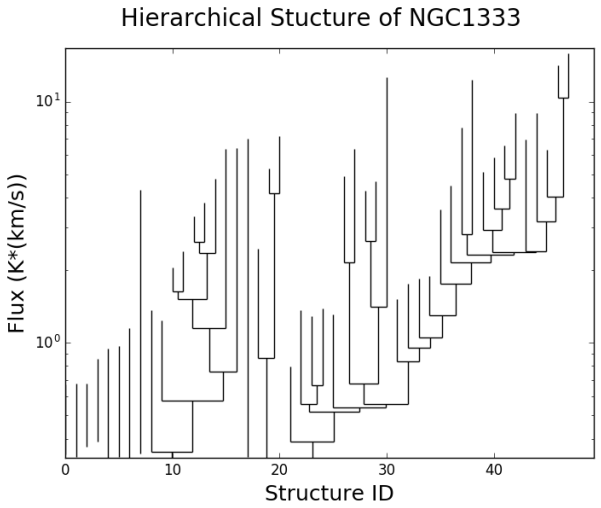

Figure 1. Dendrogram computed for NGC1333 with min_value=3σ and min_delta=2σ. The y-axis represents the flux of the structures in units of K km s^{-1}. The x-axis represents the structure index.

could easily be applied to additional SFRs in the GAS dataset to accurately outline their hierarchical structures as well. Finally, we conducted preliminary analyses on each region to assess initial hypotheses about their stability, filamentary orientations, and abundances of stellar/pre-stellar cores.

2. DATA ANALYSIS/METHODS

Dendrograms establish structural hierarchy by mapping the structures of a data set as if they are components of a tree. The smallest-scale structures are classified as 'leaves' and are placed at the top of the hierarchy. With respect to the integrated intensity maps used in this study, leaves represent the brightest, densest features within the images. In maps of SFRs, these structures are likely indicative of stellar or pre-stellar cores. Intermediate structures with sizes between the smallest and largest-scales are identified as 'branches'. Per the corollary of this name, 'branches' are the structures connecting 'leaves' to the largest-scale structures, known as 'trunks'. Within the hierarchy, 'branches' are are placed between 'leaves' and 'trunks'. As previously mentioned, 'trunks' represent the largest structures in a region and are thus placed at the bottom of the hierarchy. 'Trunks' represent large groupings of 'leaves' and, in the case of SFRs, represent the largest collections of gas, either along filaments or in clusters, within which the smaller structures are located. See Figure 1 for an example dendrogram.

To understand how we developed a preferred parameter set to generate our dendrograms, it is important to know the key parameters necessary to make them. The three key parameters are 'min_value', 'min_delta', and 'min_npix. 'min_value' indicates the minimum intensity value necessary for a pixel to be considered for inclusion in the hierarchical analysis. This parameter is essential for filtering out noise in the 0^{th} moment maps such that all structures included in the dendrograms are real. 'min_delta' indicates the required minimum difference in intensity between neighboring structures for the structures to be considered independent from one another. This parameter is the most significant in terms of identifying the hierarchy of structures in an SFR because it determines how every structure in the region should be classified relative to its neighbors. 'min_npix' simply represents the minimum number of pixels necessary for a structure to be considered independent.

In terms of identifying optimal values for these parameters, we conducted a straight-forward analysis of dendrograms made with a wide range of parameter sets by making use of the statistics generated for each diagram by the *astrodendro* package. For this analysis, we controlled two of the three key parameters while varying the remaining parameter.

We did not conduct this analysis for 'min_npix' because its required value is only decided by the number of pixels within the area of the beam used to conduct the GAS observations. To calculate this value, we simply divided the beam area by the area of a pixel. This required a conversion between the full width at half maximum (FWHM) of the beam, which is 31", to a solid angle, Ω_A. This conversion is listed in Equation 1.

$$\Omega_A = \frac{\pi * FWHM^2}{4 * ln(2)} \tag{1}$$

The area of a pixel in the GAS data is $77.42"^2$ pixel^{-1}. Dividing Ω_A by the pixel area yielded a final value for 'min_npix' of $\sim$14 pixels.

Optimizing 'min_value' and 'min_delta' required a more detailed analysis of the dendrograms generated by varying each parameter. Our baseline for these parameters was the median rms (σ) value of each region which we calculated from the rms maps made from the GAS data reduction pipeline. To narrow down ideal values for these variables, we generated several dendrograms with various values for the parameter of interest, kept 'min_npix' constant, and chose a reasonable value for the control variable. For the variable of interest, we iterated over a range of values from σ to 10σ and recorded a number of statistics (number of objects, number of leaves, and median leaf size) from each dendrogram. We then plotted the values of these statistics to look for trends in how accurately the program was defining the hierar-

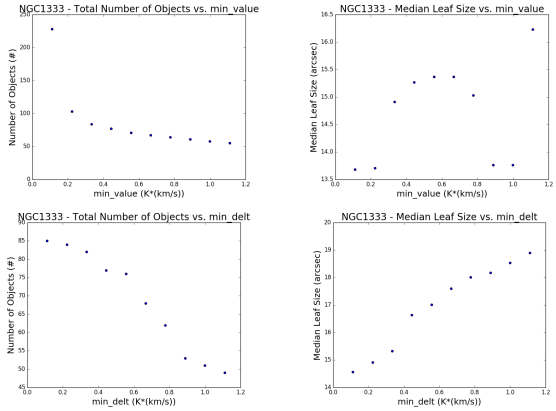

Figure 2. (Top left) Fig. 2a: Total number of objects generated by *astrodendro* for NGC1333 from min_value = σ to 10σ. (Top right) Fig. 2b: Median size of leaves generated for same dendrograms used in Fig. 2a. For 2a and 2b, min_delta was controlled as 2σ for all dendrograms. (Bottom left) Fig. 2c: Total number of objects generated by *astrodendro* for NGC1333 from min_delta = σ to 10σ. (Bottom right) Fig. 2d: Median size of leaves generated for same dendrograms used in Fig. 2c. For 2c and 2d, min_value was controlled as 3σ for all dendrograms.

chical structure of each region. Examples of these plots generated for NGC1333 are shown in Figure 2.

This method of selecting optimal parameters is more advantageous than simply selecting high multiples of σ because, if the parameter values are too high then you may be excluding real structures that are faint or small. If the parameters are too low, then the dendrograms will not be selective enough and will likely include noisy structures into the hierarchy.

We were also interested in understanding how we could utilize dendrograms to preliminarily understand more detailed aspects of star formation in these regions. One aspect we investigated was the stability of the SFRs. To address this, we thought it would be valuable to examine, among all structures identified by the dendrograms, a potential relationship between structure size and aspect ratio by plotting these statistics against one another. If most 'leaves' in these SFRs (i.e. structures with small sizes) primarily had aspect ratios near unity, this may indicate these potential stellar cores are gravitationally stable. One might expect for a small structure surrounded by larger accumulations of gas to be dominated by the "weight" of these surroundings and tend to be more round. Additionally, we were interested in the orientation of the 'leaves' with respect to the other structures in each region to determine if they tend to align with their surrounding larger structures (i.e. extended filaments). We accomplished this by plotting histograms of leaf position angles over histograms of the position angles of all structures, including leaves, in each region to look for maxima at potentially "preferred" angles. Finally, we plotted contours of the 'leaves' in each region onto their respective 0^{th} moment maps to inspect if the smallest structures identified by the dendrograms agreed with our ideas about where stellar cores should form in these regions. This analysis doubled as an evaluation of the parameter set we chose to make our final dendrograms with as this would reveal how accurately the program was dissecting the hierarchical structure of each region.

3. RESULTS

After analyzing the dendrogram statistic plots shown in Figure 2, and for the other regions not shown, we decided to select the following final values for the previously undefined parameters: min_value = 3.5σ and min_delta = 2.5σ. As mentioned before, 'min_npix' was determined by the intrinsic size of the beam used to conduct the GAS observations.

Our optimal 'min_value' was selected after analyzing the trends in Figures 2a and 2b. It is clear from Figure 2a that, for σ, the number of objects included in the dendrogram made with this parameter is significantly higher than for any other 'min_value'. This indicates a large population of non-real structures was included in the hierarchy, resulting in an inaccurate dendrogram. This is further proven by the sharp drop in this total for the slight increase to 2σ because the number of structures decreased by $\sim$50%. From 3σ to 10σ, the number of objects decreased almost linearly which revealed that the "ideal" parameter lied within this range. Although high multiples (i.e. 4 to 10) of σ certainly exclude noise from the resulting dendrograms, selecting a value in this range runs one the risk of excluding faint emission that may be important to the hierarchy. Figure 2b cements those conclusions, particularly for σ and 2σ, because the median leaf size is distinctly low for these values. This is indicative of the noisy small-scale structures included in these dendrograms as they are small and have low intensities (i.e. detectable by a low min_value) at the edges of the 0^{th} moment maps. The median leaf size is generally constant for 3-7σ which agrees with the "ideal" range we identified from Figure 2a. We are unsure as to what the sharp drop in median leaf size after 7σ indicates, as one would expect the value to increase as more small structures are excluded, but it potentially merits a closer inspection in a later study. From this analysis, we concluded that 3.5σ would be a reasonable value for which noise would be excluded from dendrograms, but fainter emission would not be overlooked.

Our optimal 'min_delta' was selected after analyzing the trends in Figures 2c and 2d as we did for 'min_value'. The nature of 'min_delta', as it applies to generating dendrograms, is more closely tied to the size of structures included in the hierarchy rather than the amount of identified structures. As such, Figure 2 shows a less drastic shift in the total number of objects as 'min_delta' increased. Low values for this parameter impose a less "strict" mandate for considering a structure as independent from its neighbors so the general decreasing trend in this plot is expected. After $\sim 5\sigma$ the number of objects decreased at a faster rate than for 1-4σ which is again a sign that these higher values prohibit small structures from inclusion in the regional hierarchy. By the same token, the lowest values of σ and 2σ are too lenient and allow non-real structure to be considered relevant to the region which should not be the case. This conclusion is verified by the median leaf size versus 'min_delta' comparison in Figure 2d. Changes made to 'min_delta' are better reflected in this plot as this parameter directly influences the acceptable structure size for dendrograms. There is a distinct increase in leaf size after 3σ that reveals the smallest features in the region are not considered by the dendrogram. Therefore, our ideal range for 'min_value' ended at 2-3σ so we chose to select 2.5σ as our final value.

To conduct our preliminary analysis of the stability of the DR1 regions, we created size versus aspect ratio plots to potentially identify trends on the smallest and largest scales. The plots made for this analysis for each region are shown in Figure 3.

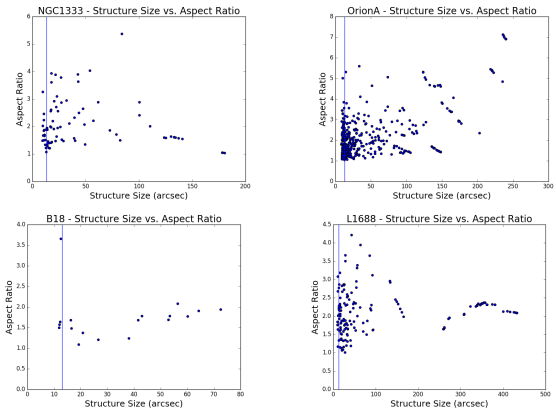

Figure 3. (Top left) Fig. 3a: Size vs. aspect ratio plot for NGC1333. (Top right) Fig. 3b: Size vs. aspect ratio plot for OrionA. (Bottom left) Fig. 3c: Size vs. aspect ratio plot for B18. (Bottom right) Fig. 3d: Size vs. aspect ratio plot for L16888. The blue line indicates the gaussian width size of the GBT beam. Each plot was made with the final optimized parameters.

Throughout all of the regions, we did not find a correlation between the size of a structure and its aspect ratio. One might claim that these plots indicate larger structures may be less likely to be compact or round. However, there is also a large spread amongst the leaves so it is difficult to determine if there is a trend among their aspect ratios despite being primarily clustered around lower values. An interesting feature to note in these plots, particularly for Orion A, is the local clusters of points at larger structure sizes. This is likely due to the dendrogram software connecting components of large structures which have very similar intensities and sizes and thus are grouped together in the hierarchy. As for some structures having sizes less than the beam size (pictured in Figure 3 as a constant blue line), this is likely due to some small abnormally-shaped structures satisfying the 'min_npix' criteria while still being smaller than the beam size.

To examine the orientation of 'leaves' with respect to all structures in each region, we made histograms of the position angles for 'leaves' (shown in red) and placed them over histograms of the position angles for all structures identified by the dendrogram (shown in blue). The plots made for this analysis for each region are shown in Figure 4.

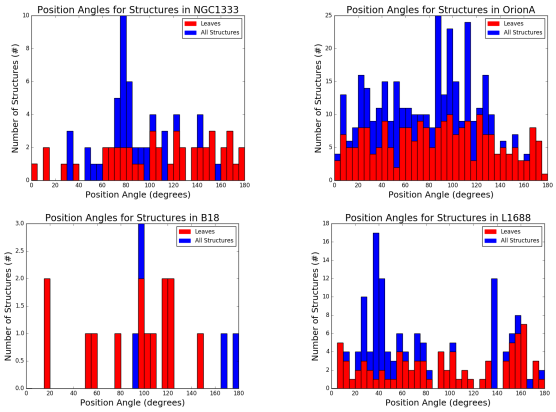

Figure 4. (Top left) Fig. 4a: Distribution of structure position angles for NGC1333. (Top right) Distribution of structure position angles for OrionA. (Bottom left) Fig. 4c: Distribution of structure position angles for B18. (Bottom right) Fig. 4d: Distribution of structure position angles for L16888. The position angle distribution for the 'leaves' is shown in red. The position angle distribution for all structures in the region is shown in blue. Each plot was made with the final optimized parameters.

Across all regions, we again see little to no correlation between the orientation of 'leaves' and the orientation of all structures. This roughly illustrates that the smallest structures in each region seem to have no pre-

ferred orientation despite being located primarily within larger 'branches' and 'trunks' that one might expect to influence their position. If we analyzed just the leaf histograms, we would see virtually no trends or maxima that may indicate a particular group of leaves are all oriented similarly.

To evaluate the accuracy of our optimized parameters and visualize the 'leaf' structures identified by our dendrograms, we plotted contours of the 'leaves' for each region on their respective 0^{th} moment maps. These figures are shown in Figure 5.

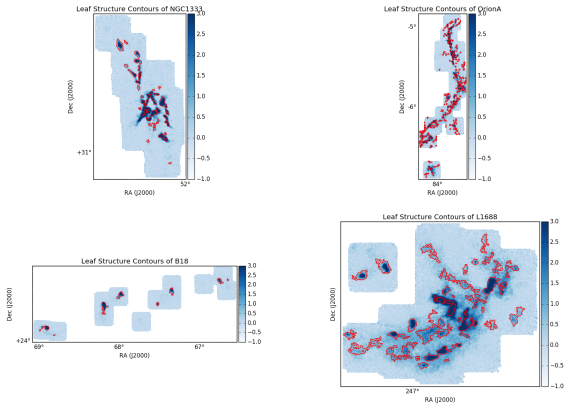

Figure 5. (Top left) Fig. 5a: 'Leaf' contours for NGC1333. (Top right) Fig. 5b: 'Leaf' contours for Orion A. (Bottom left) Fig. 5c: 'Leaf' contours for B18. (Bottom right) Fig. 5d: 'Leaf' contours for L1688. Each plot was made with the 'leaves' from the final optimized dendrograms.

This is among the best ways to visualize what, and how accurately, the dendrogram software is evaluating structures for its hierarchical analysis of SFRs. For the DR1 regions used in this study, it appears that the final parameters we chose work well to generate accurate dendrograms. This is highlighted by these contour plots because there are almost no extraneous small structures at the map edges so any noise is correctly being ignored while the smallest and densest features are included in the dendrograms. It is possible that some of the structures in the lower left of the Orion A map (Figure 5b) could be contributed by noise since there may be non-negligible rms variations in this portion of the map due to variations in the weather when this section was observed. More likely than not though, there is simply a high density of small scale structures located along the end of this bottom filament. As anticipated, it appears that the dendrogram 'leaves' correspond closely with the densest and most compact parts of each region which makes these structures ideal candidates for a future analysis of the stellar core population in each region.

4. CONCLUSION & FUTURE DIRECTION

We present a detailed analysis of the utility of the dendrogram technique for mapping the hierarchical structure of the star-forming regions involved in DR1 of GAS. We find that it is essential to optimize the parameters required by the *astrodendro* package to create the most accurate maps of these hierarchies. The statistics recorded by *astrodendro* also provide tools for conducting preliminary analyses on significant features of SFRs.

The dendrogram technique could be useful for virial analyses of both small and large-scale structures, particularly in conjunction with the 0^{th} moment maps, which may give rough estimates of the column density along particular lines-of-sight. These column densities may provide an indication of structure mass which, when paired with velocity information from the PPV cubes, could enable one to constrain virial parameters on a structure-by-structure basis.

Additionally, it would be interesting to compare the 'leaves' found by the dendrograms with potential stellar cores identified from companion continuum data (Ronan et al. 2018, in prep) released as part of the *JCMT Gould Belt Legacy Survey* (JCMT GBLS) conducted with the *Herschel Space Observatory*. Friesen et al. (2017) found that the emission detected with the tracers used by GAS (NH_3) and the JCMT GBLS (dust continuum) matched quite closely, therefore the dendrogram 'leaves' likely correspond well with stellar cores in the DR1 SFRs.

The National Radio Astronomy Observatory is a facility of the National Science Foundation operated under cooperative agreement by Associated Universities, Inc. This research made use of Astropy, a community-developed core Python package for Astronomy (Astropy Collaboration, 2018). This research made use of astrodendro, a Python package to compute dendrograms of Astronomical data (http://www.dendrograms.org/)

REFERENCES

André, P., Francesco, J. D., Ward-Thompson, D., et al. 2014, in Protostars and Planets VI (University of Arizona).

Friesen, R. K., Pineda, J. E., co-PIs, et al.\2017, ApJ, 843, 63.

Rosolowsky, E. W., Pineda, J. E., Kauffmann, J., et al.\2008, ApJ, 679, 1338.